Lens Shape and Refractive Index Distribution in Type 1 Diabetes

Adnan,[1,2] James M. Pope,[2] Farshid Sepehrband,[3] Marwan Suheimat,[1,2] Pavan K. Verkicharla,[1,2] Sanjeev Kasthurirangan,[4] and David A. Atchison[1,2]

[1]School of Optometry & Vision Science, Queensland University of Technology, Brisbane, Australia
[2]Institute of Health and Biomedical Innovation, Queensland University of Technology, Brisbane, Australia
[3]Centre for Advanced Imaging, University of Queensland, Brisbane, Australia
[4]Abbott Medical Optics, Inc., Milpitas, California, United States

Correspondence: David A. Atchison, School of Optometry & Vision Science and Institute of Health & Biomedical Innovation, Queensland University of Technology, 60 Musk Avenue, Kelvin Grove, Q, 4059, Australia; d.atchison@qut.edu.au.

Submitted: January 11, 2015
Accepted: May 22, 2015

Citation: Adnan, Pope JM, Sepehrband F, et al. Lens shape and refractive index distribution in type 1 diabetes. *Invest Ophthalmol Vis Sci*. 2015;56:4759–4766. DOI:10.1167/iovs.15-16430

Purpose. To compare lens dimensions and refractive index distributions in type 1 diabetes and age-matched control groups.

Methods. There were 17 participants with type 1 diabetes, consisting of two subgroups (7 young [23 ± 4 years] and 10 older [54 ± 4 years] participants), with 23 controls (13 young, 24 ± 4 years; 10 older, 55 ± 4 years). For each participant, one eye was tested with relaxed accommodation. A 3T clinical magnetic resonance imaging scanner was used to image the eye, employing a multiple spin echo (MSE) sequence to determine lens dimensions and refractive index profiles along the equatorial and axial directions.

Results. The diabetes group had significantly smaller lens equatorial diameters and larger lens axial thicknesses than the control group (diameter mean ± 95% confidence interval [CI]: diabetes group 8.65 ± 0.26 mm, control group 9.42 ± 0.18 mm; axial thickness: diabetes group 4.33 ± 0.30 mm, control group 3.80 ± 0.14 mm). These differences were also significant within each age group. The older group had significantly greater axial thickness than the young group (older group 4.35 ± 0.26 mm, young group 3.70 ± 0.25 mm). Center refractive indices of diabetes and control groups were not significantly different. There were some statistically significant differences between the refractive index fitting parameters of young and older groups, but not between diabetes and control groups of the same age.

Conclusions. Smaller lens diameters occurred in the diabetes groups than in the age-matched control groups. Differences in refractive index distribution between persons with and without diabetes are too small to have important effects on instruments measuring axial thickness.

Keywords: equatorial diameter, lens, lens thickness, diabetes type 1, ocular parameters, refractive index distribution, lens dimensions

We have previously conducted a study on the eyes of people with type 1 diabetes. This included consideration of a variety of ocular parameters including lens surface radii of curvature and powers, anterior corneal asphericity, lens central thickness, lens equivalent refractive index, lens equivalent power, and pupil size and position.[1] We also considered the effects of type 1 diabetes on accommodation,[2] ocular straylight, and lens yellowing.[3] The diabetic participants in the study exhibited low levels of the classic triad of diabetes complications—neuropathy, retinopathy, and nephropathy. Differences between the diabetes group and an age-balanced control group indicated that diabetic eyes appeared as older versions of normal eyes. Compared with the controls, diabetic eyes had smaller anterior chamber depths, more curved lenses, greater lens axial thicknesses, lower lens equivalent index, greater lens yellowing, and higher ocular straylight. However, there was no apparent acceleration of the changes with age that have been found in other studies for the parameters of lens yellowing,[4,5] lens thickness,[6,7] lens radii of curvature,[6,7] and lens equivalent refractive index.[7] We consider that this is due to the low levels of complications in our diabetes group.

The decrease in lens equivalent index in diabetes[7] might be due to a change in refractive index distribution, such as occurs in aging, or to an overall decrease in refractive index throughout the lens. If the lens shape characteristics (at baseline or during accommodation) are not affected, then refractive index could explain the reduction in accommodation with diabetes. If lens shape characteristics lead to reduced accommodation with diabetes, it is possible that there may be a neural component, although there may also be contributions due to the changed architecture of the lens and its supporting structures.

Lens equatorial diameter increases with aging according to Kasthurirangan et al.,[8] but not Strenk et al.[9] No information is available on lens diameters in diabetes to evaluate the finding that diabetic eyes appear to be older versions of normal eyes.

In this paper, we report on the shape, size, and refractive index distribution of the diabetic in vivo lens determined using magnetic resonance imaging (MRI).[10,11] The study involved subsets of our diabetes and nondiabetes participants for whom biometric measurements have been reported previously.[1] Magnetic resonance imaging has the advantage over optical-based techniques of not being affected by variations in

Table 1. Characteristics of Participants for Lens Dimensions and Refractive Index Distribution, Data Expressed as Mean ± Standard Deviation

	People With Diabetes	Controls	*P* Value
Number of young participants	7	13	
Number of older participants	10	10	
Young group, mean ± SD, age range, y	23 ± 4, 20–30	24 ± 4, 20–29	
Older group, mean ± SD, age range, y	54 ± 4, 48–59	55 ± 4, 50–61	
Young group, sex, F/M	2/5	7/6	
Older group, sex, F/M	6/4	6/4	
Young group, spherical equivalent refraction, D	−0.39 ± 0.78	−0.72 ± 0.65	0.32
Older group, spherical equivalent refraction, D	−0.06 ± 0.87	−0.36 ± 0.79	0.62
Young group, objective amplitude of accommodation, D	3.8 ± 1.3	6.1 ± 0.7	**0.00**
Young group, subjective amplitude of accommodation, D	5.2 ± 1.2	8.0 ± 1.2	**<0.01**
Young group, MRI lens equatorial diameter, mm	8.68 ± 0.47	9.53 ± 0.21	**0.00**
Young group, MRI axial lens thickness, mm	3.93 ± 0.27	3.58 ± 0.07	**0.02**
Young group, MRI lens center refractive index	1.400 ± 0.006	1.403 ± 0.005	0.42
Young group, MRI lens anterior axial thickness, mm	1.22 ± 0.27	1.13 ± 0.09	0.34
Young group, MRI lens posterior axial thickness, mm	2.71 ± 0.11	2.45 ± 0.11	**0.00**
Older group, MRI lens equatorial diameter, mm	8.63 ± 0.40	9.27 ± 0.34	**0.01**
Older group, MRI lens axial thickness, mm	4.61 ± 0.46	4.10 ± 0.24	**0.04**
Older group, MRI lens center refractive index	1.397 ± 0.004	1.398 ± 0.004	0.55
Older group, MRI lens anterior axial thickness, mm	1.67 ± 0.19	1.37 ± 0.20	**0.03**
Older group, MRI lens posterior axial thickness, mm	2.94 ± 0.36	2.72 ± 0.09	0.20
Young group, HbA_{1c}, %	7.60 ± 0.85	4.95 ± 0.16	**<0.001**
Older group, HbA_{1c}, %	7.92 ± 0.71	5.10 ± 0.20	**<0.001**
Young group, diabetes duration, y	17 ± 4	-	
Older group, diabetes duration, y	30 ± 9	-	

Significant *P* values are **bold**. HbA_{1c}, glycated hemoglobin.

refractive index. Refractive index distributions measured with MRI can be used to determine whether the accuracy of instruments that assume a fixed index inside the lens, such as the Haag-Streit Lenstar,[12] may be affected by variations in index distribution in diabetes.

Methods

Participants

The participants were a subgroup of a study on the optics of the eyes of people with type 1 diabetes. The majority were recruited from the Longitudinal Assessment of Neuropathy in Diabetes using novel ophthalmic Markers (LANDMark) study at the Institute of Health and Biomedical Innovation.[13] As mentioned above, all participants with diabetes recruited through LANDMark had low levels of the classic triad of diabetic complications.

Participants with and without diabetes were subdivided into young (18–30 years) and older (47–60 years) age groups (see details in Table 1). As well as meeting the selection criteria provided elsewhere[1] and clinical MRI scanning criteria, participants with diabetes in the young group had at least 2 diopters (D) of amplitude accommodation, and participants in the older group had at least 10 years of diabetes duration. Female participants were advised not to use eye makeup (including mascara) on the day of experiment to avoid artifacts that arise from the high magnetic susceptibility properties of mascara. For participants with diabetes, insulin pumps were removed, blood glucose levels were measured, and those with high levels were advised to inject insulin and were rested for at least 15 minutes before scanning.

The research adhered to the tenets of the Declaration of Helsinki. The experimental protocol was approved by the Queensland University of Technology and University of Queensland human ethics review boards. All participants were required to give written consent and to complete a standard questionnaire in order to exclude participants with heart pacemakers, aneurism clips, or other metallic implants whose function might be affected by the magnetic field of the MRI system or cause local radiofrequency heating or image distortion, and to exclude those who might have metal fragments in the eye or head.

MRI: Basic Procedures

Magnetic resonance imaging was used to measure the lens refractive index distribution and lens diameter using a 3 Tesla (Siemens Trio; Siemens, Erlangen, Germany) clinical scanner in the Centre for Advanced Imaging at the University of Queensland, Australia.

During the MRI procedure, participants were positioned supine on the patient table and heads were stabilized with padding. Participants were asked to focus (via an adjustable mirror) on a white Maltese cross fixation target on a black background that was projected onto a translucent screen at the end of the magnet bore at approximately 0.93 m from the eye. A standard 4.0-cm (Siemens) circular receive-only surface coil was taped over the examined eye so that the target was visible through the coil. A thin spacer made from self-adhesive felt, glued to the surface of the coil body, was used to minimize skin contact with the coil in order to protect against localized radiofrequency heating. The nonexamined eye was occluded using an eye patch. Participants were instructed to avoid head movement, to focus on the fixation target, and to minimize blinking during data acquisition. They were advised to blink and/or close their eyes between data acquisitions to avoid eye dryness. Where refractions were outside the range ±0.50 D (in three cases), a suitable lens was attached to the 20-mm-thick surface coil on the opposite side from the participant's eye.

MRI: Imaging Protocols

Following localizer scans to locate the position of the eye in the center of the field of view (FOV), multislice fast spin echo (FSE)

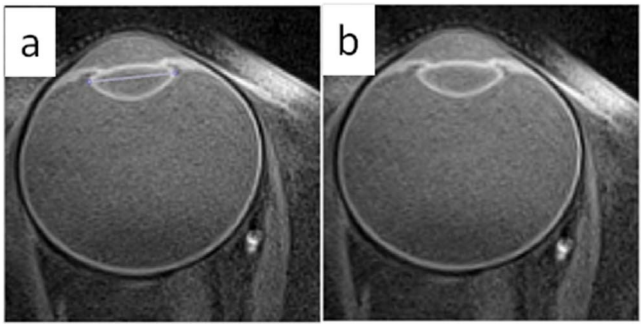

FIGURE 1. Right eye T_2-weighted MSE image of a 28-year-old nondiabetic participant showing eye rotation procedure for analysis. (**a**) A *line* is drawn through the equatorial axis of the lens, and (**b**) the desired eye rotation is achieved.

images (64-mm FOV; 256 × 256 matrix; 2-mm slice thickness (no gaps); repetition time (TR) = 4000 ms; echo time (TE) = 16 ms; echo train length 12, imaging time 128 seconds) were obtained in both axial and sagittal planes, giving in-plane resolution of 0.25 mm. A single-slice multiple spin echo (MSE) sequence (64-mm FOV; 256 × 256 matrix; 2-mm slice thickness; TR = 2000 ms; 4 echoes: TE = 12.5/25/37.5/50 ms; imaging time 4.5 minutes) was used to acquire data both for measuring lens dimensions and for calculating the refractive index distribution through the lens.[10,11,14] The FSE images were used only to ensure that the single slice was placed through the symmetry axis of the lens, using the center slice from the sagittal FSE image to identify this axis.

In MRI of the eye lens, the proton transverse or spin-spin relaxation rate ($R_2 = 1/T_2$) is proportional to the concentration of macromolecules (mainly crystallin proteins) in the lens, which in turn determines the refractive index.[14] An MSE sequence is used to map the R_2 distribution through the lens, by fitting the decay of pixel signal intensity S with echo time TE for each image voxel in the lens to the single exponential decay equation

$$S(TE) = S_0 e^{-R_2 TE}, \quad (1)$$

where S_0 is the signal intensity extrapolated to $TE = 0$ (the signal corresponding to the equilibrium or steady state magnetization). The R_2 map can then be transformed to a refractive index map at 589-nm equivalent wavelength of light, using the calibration equation[10,11,14]

$$n = 1.3554 + 1.549 \times 10^{-3} R_2 - 6.34 \times 10^{-6} R_2^2, \quad (2)$$

where n is refractive index.

A normalized refractive index distribution can be defined along the axis and equator of the crystalline lens according to[10,11,15]

$$n(r) = C_0 + C_p r^p, \quad (3)$$

where r is the normalized distance from the lens center ($r = 0$ at the center and $r = 1$ at the periphery), C_0 is the index at the lens center, C_p is the difference in refractive index between the lens center and periphery, and the exponent p characterizes the gradient refractive index rate of change. Along the optical axis, the normalized optical path [OP] from the lens center to the surface is

$$[OP] = \int_0^1 n(r)dr = \int_0^1 (C_0 + C_p r^p)dr = \left[C_0 r + C_p r^{p+1}/(p+1)\right]_0^1 = C_0 + C_p/(p+1), \quad (4)$$

which is the average index n_{av} since the normalized true path is 1.0. If uncertainties are known in the individual parameters, such as might be given by standard errors when fitting to Equation 3, the uncertainty in Δn_{av} is given by

$$\Delta n_{av} = \Delta C_0 + \frac{\Delta C_p}{p+1} - \frac{\Delta p C_p}{(p+1)^2}. \quad (5)$$

MRI: Data Processing

Image analysis was performed using custom-built software written in Matlab (version R2011; Mathworks, Natick, MA, USA). Four steps were involved in analysis of the image to measure refractive index: rotation of the image to a common axis for all participants; segmentation of the lens from the MSE image; extraction of the refractive index map; and selection of axial and equatorial lens refractive index profiles.

For rotation, a straight line was drawn by the user along the equatorial axis using the computer mouse (Fig. 1a). The software calculated the angle between the line drawn by the user relative to the horizontal, and the image was rotated by this angle. After rotation (Fig. 1b), a visual check was performed to confirm that the symmetry axis of the lens was aligned with the vertical; otherwise the user repeated the process until a satisfactory result was obtained.

Next, the user drew (with the mouse) a rectangular box around the lens that defined the region of interest. The analysis software identified the pixel intensity from each of the four MSE images and computed the refractive index value for each pixel using the procedure outlined in the previous section (Fig. 2a). The software automatically segmented out the lens from the rest of the image using a thresholding algorithm (Fig. 2b). Although the iris touched the anterior lens, this did not affect the process because the signal from the iris decayed much more slowly in the later echo images. Pixels corresponding to the aqueous and vitreous humors were artificially assigned a refractive index of 1.336.[11]

Due to motion and blinking in some participants, MSE images and hence refractive index maps suffered from artifacts. In order to improve signal to noise (S/N) and make comparisons between different participant groups, lens refractive index profiles were computed using the line of pixels closest to the lens axis or equatorial diameter, and also by averaging over a 3-pixel-wide band centered on these axes (Fig. 2c). For this purpose, the segmented lens was used, and the rows and columns of data in the refractive index maps that corresponded most closely to the equator and axis of the lens, respectively, were identified. As MSE images had in-plane resolution of 0.25 mm and slice thickness of 2 mm, this gave an effective voxel size of 0.375 mm^3 (3 × 0.25 × 0.25 × 2). The central refractive index was calculated as the mean refractive index over 3 × 3 pixels at the lens center (red dot in Fig. 3).

The first MSE image (TE = 12.5 ms) with the best S/N and contrast was selected to determine the lens diameter and axial thickness manually using ImageJ software (http://imagej.nih.gov/ij/; provided in the public domain by the National Institutes of Health, Bethesda, MD, USA). The equatorial diameter was measured along the equatorial diameter line between nasal and temporal edges of the lens, and the axial thickness was measured along the optical axis between the anterior and posterior edges of the lens. An anterior axial thickness was measured from the anterior edge of the lens to the center of the equatorial diameter line. Similarly, a posterior axial thickness was measured from the posterior edge to the center of the equatorial diameter line (Fig. 3).

To analyze refractive index data, lens dimensions were normalized for each individual. For the equatorial axis, the

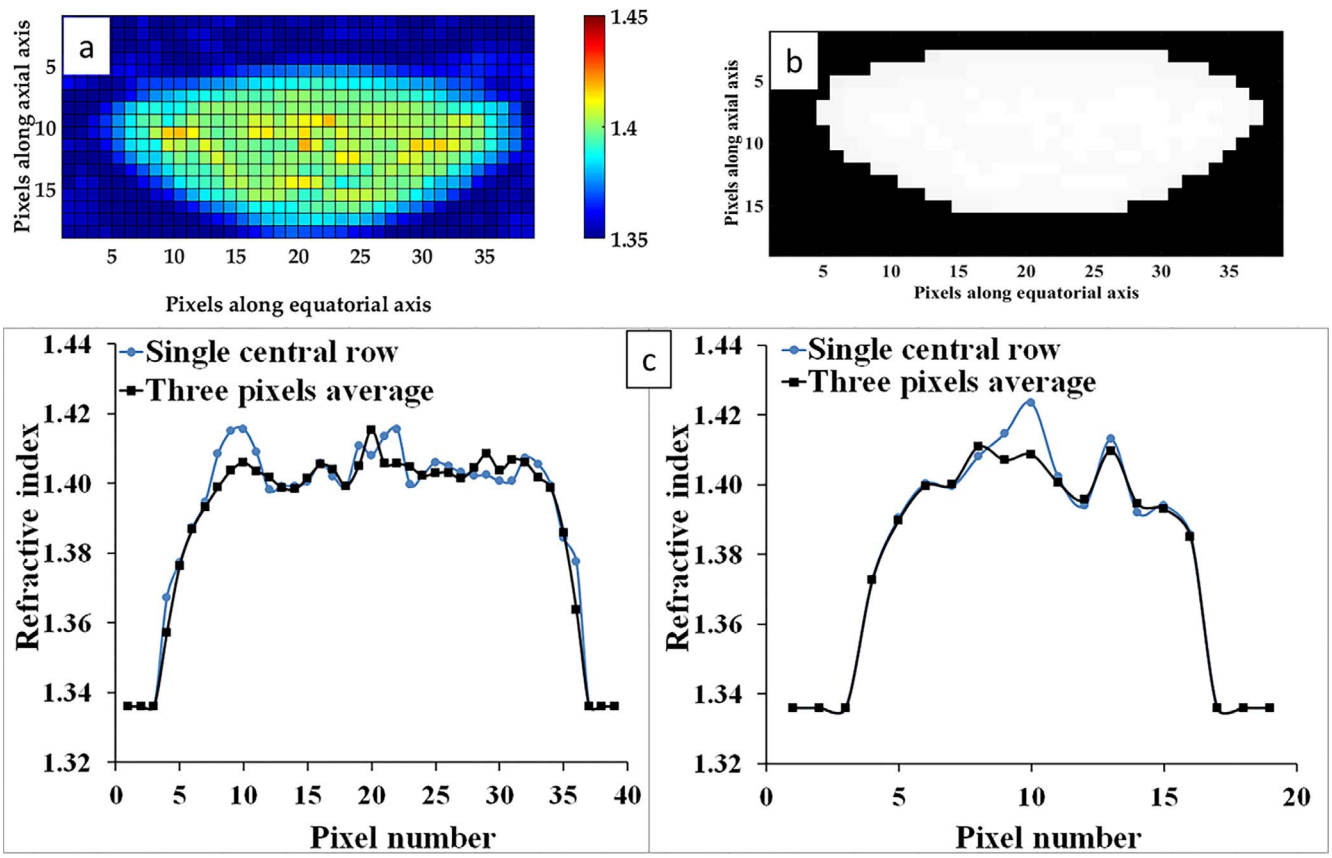

Figure 2. Schematic representation of refractive index extraction procedure. (**a**) Customized software identified equivalent pixels within the image and generated a refractive index distribution map of the lens. (**b**) A thresholding algorithm segmented the lens from the rest of the refractive index map. The vertical and horizontal axes of the figures represent pixels. (**c**) Profiles of refractive index over a central single row and averaged over three rows of pixels, plotted against pixel number (*left*) in the equatorial (temporal to nasal) direction closest to the equator (*right*) in the axial (anterior to posterior) direction closest to the lens axis. Each pixel represents 0.25 mm.

normalized dimension extended from −1 to +1. The data were folded about the optical axis to give a normalized dimension 0 to +1, and group data were fitted according to Equation 3. The optical axis dimension was normalized by two different approaches. In the first approach, normalization extended from −1 to +1 relative to the midpoint between the anterior and posterior vertices of the lens for each person. The data were folded about the midpoint (red dot in Fig. 3) to give a normalized dimension 0 to +1, and group data were fitted according to Equation 3. In the second approach, separate analyses were performed for the portions anterior and posterior to the midpoint of the equatorial diameter (blue dot in Fig. 3) with normalized dimension for each portion of 0 to +1.

Results

Participant details are given in Table 1. There were 17 participants with diabetes (7 young, 10 older) and 23 age-matched control participants (13 young, 10 older). For all but three participants, right eyes were used. Table 1 shows means of the refractive index and lens dimensional results in the four subgroups and statistical comparisons using unpaired *t*-tests between the diabetes and control participants in the young and older age groups. Figure 4 has images of typical young diabetes, young control, older diabetes, and older control participants.

Two-way ANOVAs were performed to consider the effects of diabetes and age on lens equatorial diameter, axial thickness, and center refractive indices. The diabetes group as a whole had significantly smaller equatorial diameters than the control group ($F_{1,36} = 24.5$, $P < 0.01$; mean ± 95% confidence interval [CI]: diabetes group 8.65 ± 0.26 mm, control group 9.42 ± 0.18 mm), and significantly greater axial thicknesses than the control group ($F_{1,36} = 11.9$, $P < 0.01$; mean ± 95% CI: diabetes group 4.33 ± 0.30 mm, control group 3.80 ± 0.14 mm) (Fig. 5). The center refractive indices of the diabetes and control groups were not significantly different ($F_{1,36} = 3.0$, $P = 0.09$).

Age group did not affect equatorial diameter significantly ($F_{1,36} = 0.10$, $P = 0.20$). The older group had significantly greater axial thicknesses than the young group, as was

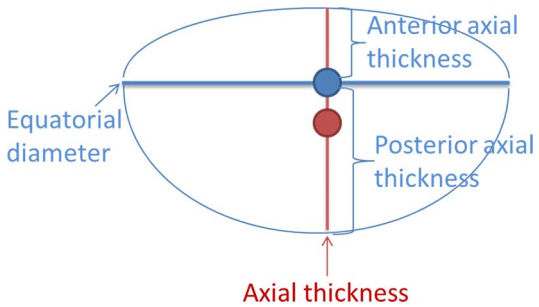

Figure 3. Lens dimensions for refractive index profiles.

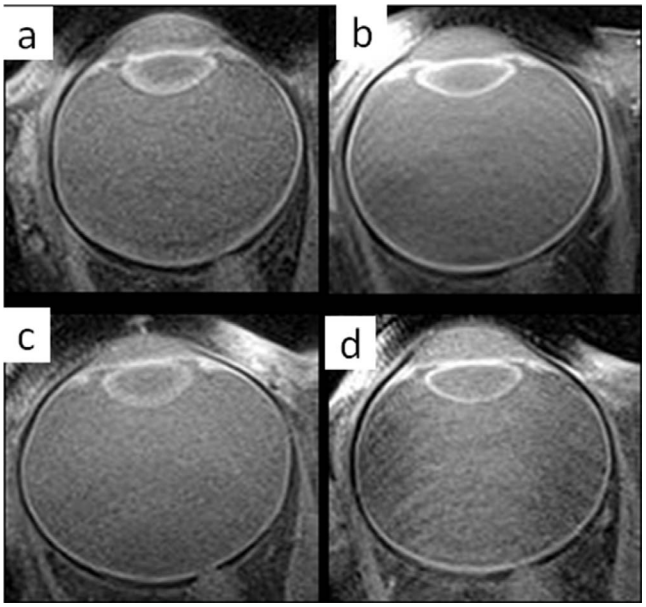

FIGURE 4. Characteristic MSE images from each of the groups: (**a**) 21-year-old (young) male with 19-year diabetes duration, (**b**) 21-year-old (young) female control, (**c**) 49-year-old (older) female with 34-year diabetes duration, and (**d**) 53-year-old (older) male control. These demonstrate smaller equatorial diameter and greater axial thickness for diabetes than for control lenses ([**a**] versus [**b**], [**c**] versus [**d**]) and greater axial thickness for older than for young lenses ([**c**] versus [**a**], [**d**] versus [**b**]).

expected from previous investigations ($F_{1,36} = 22.4$, $P < 0.01$; mean ± 95% CI: older group 4.35 ± 0.26 mm, young group 3.70 ± 0.25 mm) (Fig. 5). The older group had significantly lower center refractive indices than the young group ($F_{1,36} = 4.14$, $P = 0.04$; mean ± 95% CI: older group 1.398 ± 0.003, younger group 1.401 ± 0.004).

The combined normalized refractive index profile data of each group (young diabetes, young control, older diabetes, older control) were fitted by the power equation, Equation 3, for different directions, and the average refractive index along the axis of the lens was determined with Equation 4. Table 2 shows fitted refractive index coefficients for the equatorial diameter and for the optical axis, together with the average axial refractive index. In this table, the first normalization approach described in the section "MRI: Data Processing" was used for fitting the axial data, in which the profiles were folded about the midpoint of the lens axis and no distinction was made between the anterior and posterior segments. Table 3 shows the fitted refractive index coefficients for the optical axis obtained using the second normalization approach for fitting the axial data, in which the anterior and posterior segments are fitted separately, together with the corresponding average axial refractive index. Figure 6 shows the refractive index profiles along the equatorial diameter and the optical axis (first normalization approach), together with fits according to Equation 3.

There was considerable variation within groups. The central plateaus appeared wider for the older than for the younger groups, particularly along the equatorial diameter.

Unpaired *t*-tests were used to compare groups for each of the directions, in which the standard deviations were not assumed to be equal and Bonferroni correction was applied as there were six pairwise comparisons per direction. There were a few significant differences only (Tables 2 and 3). These involved the following: both young groups compared with both older groups: p equatorially; both young groups compared with the older diabetes group: C_0 equatorially; young diabetes group compared with both older groups: C_p axially; young diabetes group compared with older control group: C_0 axially, C_p posterior axially, and p posterior axially. There were no significant differences between diabetes and control groups of the same age.

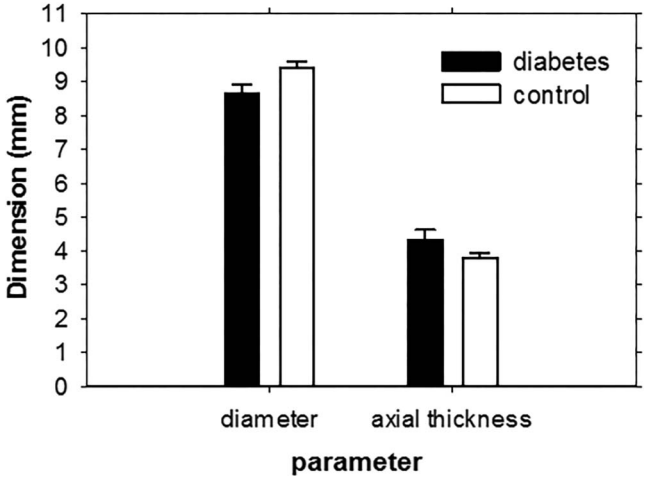

FIGURE 5. Mean lens diameters and axial thicknesses of the diabetes and control groups. *Error bars* are 95% confidence intervals of means.

DISCUSSION

The interesting finding of this study was the difference in lens shapes between the diabetes and control groups; the former had more rounded shapes with smaller equatorial diameters and greater axial thicknesses. The refractive index data within groups were highly variable. A few statistically significant differences of refractive index were found between young and older groups, although not between diabetes and control groups of the same age.

It is notable that the bright ring around the periphery of the lenses in the spin echo images of Figure 4 typically appears less prominent in the lenses of diabetic participants. This is a region of high signal intensity arising from higher water content in the outer cortex and epithelial layer compared with the lens center. As lenses age, this region of higher signal intensity tends to become more diffuse and less prominent, especially in the case of diabetic lenses. This is consistent with the hypothesis that changes with age occur earlier and are more pronounced in diabetic lenses than those of nondiabetics.

Amplitude of accommodation is smaller in people with diabetes than in people without diabetes.[2,16] The young participants in this MRI study were part of a study of amplitude of accommodation, and the mean amplitudes of these subsets of the diabetes and control groups were 3.8 D and 6.1 D by an objective technique and 5.2 D and 8.0 D by a subjective technique. The different shapes of diabetes and nondiabetes lenses may contribute to this. The unaccommodated shapes of lenses in people with diabetes mimic the accommodated shape of lenses of people without diabetes. The zonules may be exerting greater tension on the diabetic lens than on the nondiabetic lens for the unaccommodated state. This means that a particular contraction of the ciliary muscle may be less able to reduce tension on the diabetic lens so that it is less able to further change shape under the influence of its elastic capsule. The numbers for the investigation were small in this study (40 across two ages), and further investigation is

Table 2. Coefficients of Fit $n(r) = C_0 + C_p r^p$ to Refractive Index Data Along Equatorial Diameter Line and Optical Axis of Different Groups, Together With the Average Refractive Index Along the Axial Direction

Participant Group	C_0 Equator	C_p Equator	p Equator	C_0 Axial	C_p Axial	p Axial	n_{av} Axial
Young diabetes group	1.4004* (0.0010)	−0.0309 (0.0026)	2.8022*† (0.4522)	1.4016† (0.0017)	−0.0448*† (0.0061)	2.5541 (0.5621)	1.3890 (0.0054)
Young control group	1.4015* (0.0006)	−0.0432 (0.0040)	4.4812*† (0.5228)	1.3988 (0.0012)	−0.0297 (0.0027)	3.6039 (0.6518)	1.3923 (0.0027)
Older diabetes group	1.3974 (0.0006)	−0.0318 (0.0043)	8.6327 (1.5302)	1.3967 (0.0010)	−0.0281 (0.0028)	3.5286 (0.6390)	1.3905 (0.0025)
Older control group	1.3978 (0.0006)	−0.0608 (0.0123)	9.5572 (1.5638)	1.3961 (0.0010)	−0.0235 (0.0025)	4.9400 (1.0944)	1.3921 (0.0021)

Numbers in parentheses are standard errors.
* Significantly different from older diabetes group.
† Significantly different from older control group.

Table 3. Coefficients of Fit $n(r) = C_0 + C_p r^p$ to Anterior Axial and Posterior Axial Refractive Index Data of Different Groups Using the Second Approach to Normalization Along the Optical Axis

Participant Group	C_0 Anterior Axial	C_p Anterior Axial	p Anterior Axial	C_0 Posterior Axial	C_p Posterior Axial	p Posterior Axial
Young diabetes group	1.3993 (0.0040)	−0.0501 (0.0111)	2.0717 (0.8565)	1.4008† (0.0013)	−0.039† (0.0085)	5.2397 (1.5146)
Young control group	1.3995 (0.0030)	−0.0524 (0.0095)	2.3139 (0.7401)	1.3991 (0.0011)	−0.0219 (0.0031)	4.2919 (1.1320)
Older diabetes group	1.3951 (0.0018)	−0.0443 (0.0137)	4.5203 (1.6944)	1.3967 (0.0010)	−0.0237 (0.0026)	4.3872 (0.9786)
Older control group	1.4014 (0.0022)	−0.0498 (0.0088)	2.8434 (0.7970)	1.3959 (0.0010)	−0.0190 (0.0028)	5.0866 (1.4774)

Numbers in parentheses are standard errors.
† Significantly different from older control group.

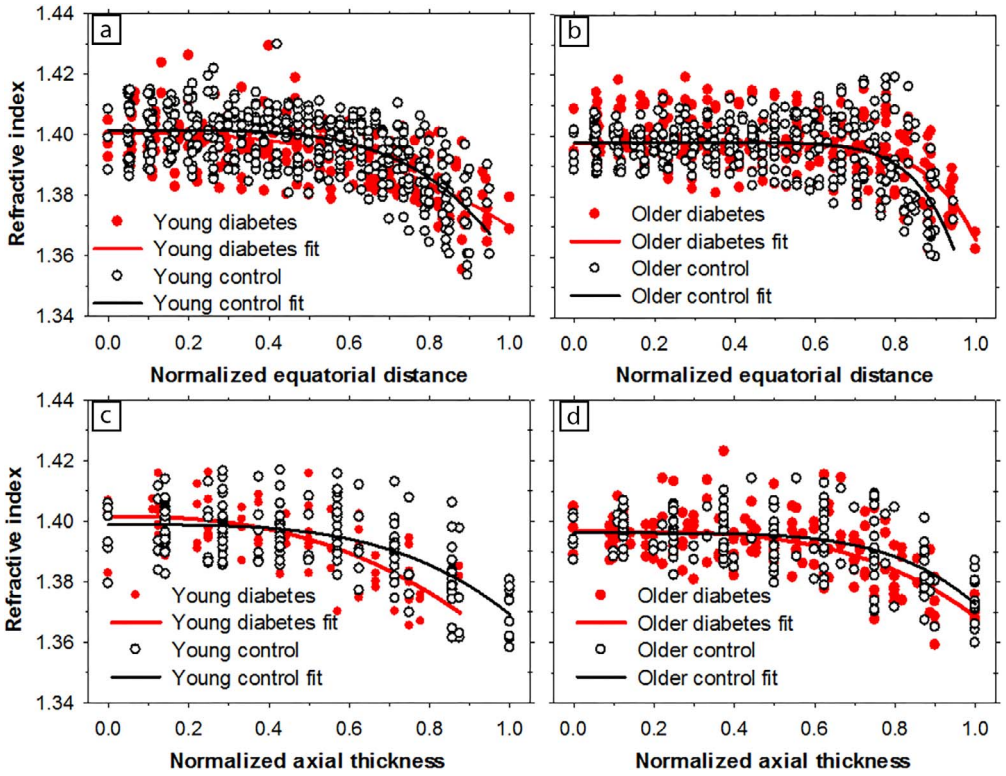

FIGURE 6. Normalized refractive index profiles for diabetes and control groups, together with fits to Equation 3: (**a**) young groups, equatorial diameter; (**b**) older groups, equatorial diameter; (**c**) young groups, axial; and (**d**) older groups, axial. The origin for the equatorial data corresponds to the *blue dot* in Figure 3, while that for the axial data corresponds to the *red dot*.

warranted to study changes in the lens diameter and movements of the zonules and ciliary muscle during accommodation.

Comparing the nondiabetic lenses in this study with the findings of Kasthurirangan et al.[11] for unaccommodated lenses, there was agreement in that there were similar axial thickness changes with age, there was no change in center refractive index with age, and the rate of decline in refractive index from center to periphery was greater along the equatorial diameter line than along the optical axis. However, there were some differences. The mean diameter in the study by Kasthurirangan et al.[11] was 0.23 mm smaller than found here, their central indices were approximately 0.007 higher, differences between center and edge refractive indices were approximately 0.005 greater, and they found significantly larger lens diameters in the older group than in the younger group whereas there was no difference in the current study.

Power fits of refractive index (Equation 3) were made to the combined data of the participants along the equatorial diameter line and optical axis in each of the groups. There were a few significant differences involving the young groups compared with the older groups, but there were no significant differences within either age group for the people with and without diabetes. Of course, the study is limited by small numbers in the groups. The age-related effects in refractive index distribution support the study by Kasthurirangan et al.[11]

The average axial refractive index had a 0.003 range between the groups, and the variation within groups (standard deviations 0.008–0.014) was much greater than the between-group variation. It is important to determine if this range of variability would affect lens thickness measurements in commercial instruments. Assuming that an instrument like the Haag-Streit Lenstar is calibrated for a lens refractive index n_{ref}, the associated optical path length is

$$OPL = d_L n_{ref}, \quad (6)$$

where d_L is the lens central thickness. If this optical path length had been determined for another lens with a refractive index n and thickness $(d_L - \Delta d_L)$ the relationship would be

$$OPL = (d_L - \Delta d_L)/n. \quad (7)$$

Δd_L, the error in central thickness given by the instrument, can be found by equating the right-hand sides of the two equations:

$$\Delta d_L = d_L\left(1 - \frac{n_{ref}}{n}\right). \quad (8)$$

If it is assumed that n_{ref} is 1.3921 and corresponds to the average axial refractive index of the older control group, the average errors for the other groups range between $-0.0022 d_L$ and $+0.0001 d_L$. If the determined thickness was 5.00 mm, errors would range between –0.012 and +0.001 mm. The precision of the Lenstar (although not necessarily the accuracy) is 0.01 mm, which is similar to the range of these errors.

Recently three-dimensional optical coherence tomography has been developed to measure lens parameters including the lens gradient index (e.g., Siedlecki et al.[17]). With the much higher resolution of OCT compared to MRI, it will be interesting if subtleties in refractive index distribution in different conditions such as diabetes can be distinguished, although like our method, this technique relies on assumptions such as the form of the gradient index.

In conclusion, we conducted a magnetic resonance imaging study of lens dimensions and lens refractive index distributions in type 1 diabetes and age-matched control groups. Smaller lens diameters occurred in the young and older type 1 diabetes groups than in the age-matched control groups. Differences in

refractive index distribution between people with diabetes and those without are too small to have important effects on instruments measuring axial thickness.

Acknowledgments

We thank the Centre for Advanced Imaging, University of Queensland, and in particular its radiographers Aiman Al Najjar and Anita Burns.

Supported by Johnson & Johnson Vision Care, Inc., Florida, United States.

Disclosure: **Adnan**, None; **J.M. Pope**, None; **F. Sepehrband**, None; **M. Suheimat**, None; **P.K. Verkicharla**, None; **S. Kasthurirangan**, None; **D.A. Atchison**, None

References

1. Adnan, Suheimat M, Efron N, et al. Biometry of eyes in type 1 diabetes. *Biomed Opt Express*. 2015;6:702–715.
2. Adnan, Efron N, Mathur A, et al. Amplitude of accommodation in type 1 diabetes. *Invest Ophthalmol Vis Sci*. 2014;55:7014–7018.
3. Adnan, Suheimat M, Mathur A, Efron N, Atchison DA. Straylight, lens yellowing and aberrations of eyes in type 1 diabetes. *Biomed Opt Express*. 2015;6:1282–1292.
4. Lutze M, Bresnick GH. Lenses of diabetic patients "yellow" at an accelerated rate similar to older normals. *Invest Ophthalmol Vis Sci*. 1991;32:194–199.
5. Davies NP, Morland AB. Color matching in diabetes: optical density of the crystalline lens and macular pigments. *Invest Ophthalmol Vis Sci*. 2002;43:281–289.
6. Sparrow JM, Bron AJ, Brown NAP, Neil HAW. Biometry of the crystalline lens in early-onset diabetes. *Br J Ophthalmol*. 1990;74:654–660.
7. Wiemer NGM, Dubbelman M, Kostense PJ, Ringens PJ, Polak BCP. The influence of diabetes mellitus type 1 and 2 on the thickness, shape, and equivalent refractive index of the human crystalline lens. *Ophthalmology*. 2008;115:1679–1686.
8. Kasthurirangan S, Markwell EL, Atchison DA, Pope JM. MRI study of the changes in crystalline lens shape with accommodation and aging in humans. *J Vis*. 2011;11:1–16.
9. Strenk SA, Semmlow JL, Strenk LM, Munoz P, Gronlund-Jacob J, DeMarco JK. Age-related changes in human ciliary muscle and lens: a magnetic resonance imaging study. *Invest Ophthalmol Vis Sci*. 1999;40:1162–1169.
10. Jones CE, Atchison DA, Meder R, Pope JM. Refractive index distribution and optical properties of the isolated human lens measured using magnetic resonance imaging (MRI). *Vision Res*. 2005;45:2352–2366.
11. Kasthurirangan S, Markwell EL, Atchison DA, Pope JM. In vivo study of changes in refractive index distribution in the human crystalline lens with age and accommodation. *Invest Ophthalmol Vis Sci*. 2008;49:2531–2540.
12. Suheimat M, Verkicharla PK, Mallen EAH, Rozema JJ, Atchison DA. Refractive indices used by the Haag-Streit Lenstar to calculate axial biometric dimensions. *Ophthalmic Physiol Opt*. 2015;35:90–96.
13. Pritchard N, Edwards K, Dehghani C, et al. Longitudinal assessment of neuropathy in type 1 diabetes using novel ophthalmic markers (LANDMark): study design and baseline characteristics. *Diabetes Res Clin Pract*. 2014;104:248–256.
14. Jones CE, Pope JM. Measuring optical properties of an eye lens using magnetic resonance imaging. *Magn Reson Imaging*. 2004;22:211–220.
15. Smith G, Atchison DA, Pierscionek BK. Modeling the power of the aging human eye. *J Opt Soc Am A*. 1992;9:2111–2117.
16. Moss S, Klein R, Klein B. Accommodative ability in younger-onset diabetes. *Arch Ophthalmol*. 1987;105:508–512.
17. Siedlecki D, de Castro A, Gambra E, et al. Distortion correction of OCT images of the crystalline lens: gradient index approach. *Optom Vis Sci*. 2012;89:709–718.

Investigative Ophthalmology & Visual Science